Improvement of an association algorithm for obstacle tracking

Abstract

This article describes a modification of an association algorithm for object tracking based on the evidence theory. This association algorithm was first developed by M. Rombaut and subsequently improved in a general way by D. Gruyer. This algorithm has been modified here in order to obtain better results when data reliability is poor. This article presents the basic concepts of the evidence theory. Then, the association algorithm developed by M. Rombaut is explained, and some examples are given to show that this algorithm fails to give the proper decision when data reliability decreases. Finally, the new algorithm is presented and the two algorithms are compared using synthetic data. In order to test the robustness of the two algorithms, they were also tested using real data coming from a CCD camera and these data can be qualified as very noisy with a reliability ranging from good to very bad.

Key words: Data Fusion, Evidence Theory , Association, Tracking.

1 Introduction

This article relates to intelligent vehicles and more precisely to making an algorithm for obstacle detection and tracking. Many European projects on intelligent vehicles are currently in progress, and before explaining the work done, here, a short description will be given of the work achieved in some of these projects.

In the Carsense project [1], the car is fitted with six sensors: two cameras in stereovision, another for lane following, a long-range radar, a short-range radar and a laser. Except for lane-keeping camera, all the sensors are dedicated to obstacle detection in front of the car. The algorithm must be able to detect many objects simultaneously. Data fusion is carried out using the evidence theory and an association algorithm for tracking is described. The aim of this project is to establish, the car environment as reliably as possible.

The aim of the Argo project [2] is to provide a driver assistance system capable of driving the car at the driver's request. The experimental car is fitted with just two stereovision cameras and one speedometer. The wheel is motorized to

allow automatic drive. Some tests were performed to compare the detection results between a single camera and two in stereovision [3].

The Autonomes Fahren project [4] is based on a car integrating a DGPS, a digital map, three lasers (one at the rear and two in the front), several short-range radars on both sides, a long-range radar and a stereovision system. Objects are detected and tracked in a Kalman filter. The car is fitted with actuators to make the driving task fully automatic.

Also worth mentioning is the development of the Adaptative Cruise Control (ACC), named Stop and Go ACC [5]. This system works with a millimeter wave radar and a lane-keeping camera. Its aim is to maintain automatically a safety distance between two vehicles in cruise control mode.

Finally, other research work on intelligent vehicles using stereovision systems can be found in [6].

The project discussed here is a part of is RaViOLi: "Radar, Vision Orientable et Lidar". In this project, three sensors are used: a long-range radar, a stereo-vision system and a Lidar. The interest of this project is to make a long-range detection system. Given that reliability decreases with increasing in ranging distance, a fusion algorithm for detection and tracking of moving objects has been developed that is still able to work when data reliability is poor.

Taking directly into account the imperfections due to each item of information and each sensor, the algorithm is based on the evidence theory [7,8]. The procedure is as follows: first, belief masses are created for each sensor, with the different measurements they provide. Then, the belief functions made from the measurements are combined and then, those from each sensor are also combined. Finally, an association algorithm gives a decision: a new object appears, the object disappears, or the object had already been detected before.

This article is organized as follows: section 2, describes the basic concept of the evidence theory. Section 3 presents the method for creating the mass sets for the different sensors and the fusion steps. Section 4, describes the association algorithm and the modifications made to improve it when detected objects are a long way ahead of the sensors. Section 5 compares the results obtained with this algorithm using synthetic and real data. Finally, possible future developments of this algorithm are indicated in section 6.

2 Evidence theory

The evidence theory was initially introduced by Dempster [7] in relation to his work on lower and upper bounds of a distribution probability family. Using this mathematical formalism, Shafer [8] shows the benefits of belief functions for modelling uncertain knowledge. The usefulness of Belief functions, as an alternative to subjective probabilities, was subsequently proved in an axiomatic way by Smets [9,10] in the *Transferable Belief Model* thus giving a clear and coherent interpretation of the subjacent concept of this theory. In this section, some mathematical elements of belief functions will be introduced. Not all of the concepts of this theory will be introduced but just those needed to understand this article. Then, an approach will be explained for using the evidence theory in the case of object association.

2.1 Basic concepts

The evidence theory is based on the assumption that, from the beginning, a set Ω called the frame of discernment is known and which is defined as follows:

$$\Omega = \{\omega_1, \omega_2, \ldots \omega_N\} \tag{1}$$

This set is composed of N exhaustive and exclusive hypotheses. From this frame of discernment, a set noted 2^Ω can be built, including the 2^N proposals A of Ω:

$$2^\Omega = \{A/A \ \subseteq \Omega\} \tag{2}$$

A belief function can be mathematically defined by a mass function (or allocation [1]), noted m defined by 2^Ω in $[0, 1]$, and that verifies:

$$\sum_{A \subseteq \Omega} m(A) = 1 \tag{3}$$

Each subset $A \subseteq \Omega$ such that $m(A) \neq 0$ is called a focal element of Ω. Thus, mass $m(A)$ represents the degree of belief allocated to the proposal A and that cannot, in the present state of knowledge, be attributed to a subset more specific than A. The belief function for which $m(\emptyset) = 0$ is called normal. In the Transferable Belief Model, the condition $\sum_{\emptyset \neq A \subseteq \Omega} m(A) = 1$ is not imposed and it is possible to have $m(\emptyset) \neq 0$. This can introduce the notion of *open world* while assuming that the belief cannot be attributed to a subset of Ω. In this case, $\emptyset$ can be interpreted as a proposal which is not in the frame of discernment Ω and that it is likely to be the solution to the problem as opposed to the *closed world* where the set Ω is assumed to be exhaustive.

[1] The term *bba* for *basic belief assignment is often found in the literature*

2.2 Dual functions

From the belief mass, other belief functions such as plausibility can be defined:

$$pl(B) = \sum_{A \cap B \neq 0} m(A) \qquad \forall B \subseteq \Omega \tag{4}$$

This function can be interpreted as the part of belief that can potentially be allocated to B taking into account the elements that do not discredit this proposal. Another belief function that is often found in the literature is the credibility function which is obtained as follows:

$$bel(B) = \sum_{A \subseteq B} m(A) \qquad \forall B \subseteq \Omega \tag{5}$$

This function represents the belief brought to the elements of that proposal. Plausibility and credibility functions are dual measures. Those measures can be viewed as lower and upper bounds of function m. In addition, the different functions pl, bel and m represent the same information but expressed in different ways. Moreover, they can be translated from one to the other thanks to the Möbius transform [11,12].

2.3 Discounting

When the information that results in the belief function is not totally reliable, it may be useful to discount this belief. In order to do that, a coefficient α is used, which represents knowledge of the source reliability. This coefficient will allow the transfer of the belief to the set Ω when the information is not totally reliable. The discounting belief function m_α, defined by a reliability coefficient α can then be deduced from m by means of the following expression:

$$\begin{cases} m_\alpha(A) = \alpha m(A) \\ m_\alpha(\Omega) = 1 - \alpha + \alpha m(\Omega). \end{cases} \tag{6}$$

2.4 Fusion of belief functions

In the evidence theory, data from distinct sources are fused using the *rule of Dempster combination*, also known as the orthogonal sum. This sum, which is commutative and associative, is defined by:

$$\forall\, A \in 2^\Omega \qquad m(A) = m_1(A) \oplus \ldots \oplus m_Q(A) \tag{7}$$

where $\oplus$ represents the combination operator. In cases of two sources noted S_i and S_j, giving respectively belief functions noted m_i et m_j, the combination can be written as follows:

$$m(C) = \frac{1}{1-K} \sum_{A \cap B = C} m_i(A).m_j(B) \tag{8}$$

where K is defined by:

$$K = \sum_{A \cap B = \emptyset} m_i(A).m_j(B). \tag{9}$$

In equation (8), the coefficient K reflects the existing conflict between two sources S_i and S_j. When this factor equals 1, the sources are in total conflict and the information cannot be fused. On the other hand, when K equals 0, the two sources totally agree. This fusion rule, deduced from the conditioning rule [13], has been criticized in several publications such as [13–15], particularly for the case of two totally conflicting sources. In order to avoid this disadvantage, Dubois and Prade [16] have defined a disjunctive and conjunctive fusion operator. Finally, another form of combination has been proposed in order to gather all the fusion operators that can be used in the evidence theory [17,18].

When comparing it to the probability theory, the evidence theory shows some advantages, the most important of which is the possibility of expressing the degree of uncertainty. In this theory, the mass assignment on a subset does not mean that the remainder automatically goes to the complement.

2.5 Measures of uncertainty

It follows from the nature of the evidence theory that it subsumes two distinct types of uncertainty [19]. One of them is called the nonspecificity. This measure is defined by the following formula:

$$N(m) = \sum_{A \subset \Omega} m(A) \cdot log_2 \mid A \mid \tag{10}$$

where $\mid A \mid$ denotes the cardinality of the focal element A. This measure, which was proven to be unique under appropriate requirements [20], expresses the uncertainty of the belief function m. It ranges from: $0 \leq N(m) \leq log_2 \mid \Omega \mid$. $N(m) = 0$ when $m(A) = 1$ ($A \subset \Omega$ and A is a singleton), corresponding to the full certainty. $N(m) = log_2 \mid \Omega \mid$ when $m(\Omega) = 1$ (total ignorance).

The second type of uncertainty captured by the evidence theory is called the

discord. This measure was defined as follows by [21]:

$$D(m) = -\sum_{A \subset \Omega} m(A) \cdot log_2[1 - \sum_{B \subset \Omega} m(B) \cdot \frac{\mid B - A \mid}{\mid B \mid}] \tag{11}$$

This measure gives the mean conflict (expressed by the logarithmic transformation) among evidential claims within each given body of evidence. Note that the following part:

$$\sum_{B \subset \Omega} m(B) \cdot \frac{\mid B - A \mid}{\mid B \mid} \tag{12}$$

expresses the sum of individual conflicts of evidential claims with respect to a particular set A.

After this introduction to the basic concepts of the evidence theory, the next section deals with the creation of masses, adapted to the present application, using information from the different sources.

3 Creation of masses

In an intelligent vehicle, objects are detected by sensors installed in the vehicle. From these sensors used for RaViOLi, the kind of information is known and is expressed in terms of (distance;angle): $(\rho; \Theta)$. Moreover, it is considering that using a radar, the speed can be obtained independently of the angle and the distance, by Doppler effect. In addition, the dimensions of the object re also available.

The aim is to track vehicles. Therefore, it must be possible to find them from one moment to another. All the available information is used to create several mass sets indicating the relations that exist between perceived objects at time t and those known at time $t-1$. The term X_i denote the objects Perceived ($i = 1 : NbP$) at time t by the sensors and Y_j the Known objects ($j = 1 : NbK$). The known objects are perceived objects from the previous sample time that were stored in memory.

In a first stage, The frame of discernment must be defined as a basis for the work. Two hypotheses have been chosen: $\Omega = \{(X_i R Y_j); (X_i \overline{R} Y_j)\}$. Either the perceived object is the same as the known one (in relation:$(X_i R Y_j)$), or it is not in relation :$((X_i \overline{R} Y_j))$ [22].

The first step consists in creating belief functions using the information. A different mass set is built for each usable item of information from each sensor.

The mathematical equations of the mass set, that can be used to determine whether objects are in relation or not, is based on a negative exponential

introduced by Denoeux [23]:

$$
\begin{aligned}
m_{i,j}(X_i R Y_j) &= \alpha_0 \cdot exp^{(-e_{i,j}^2)} \\
m_{i,j}(X_i \overline{R} Y_j) &= \alpha_0 \cdot (1 - exp^{(-e_{i,j}^2)}) \\
m_{i,j}(\Omega_{i,j}) &= 1 - \alpha_0
\end{aligned}
\tag{13}
$$

where $e_{i,j}$ is the variation between two items of information (distance, angle, or speed) from perceived X_i and known Y_j objects. α_0 is a coefficient that characterizes the sensor reliability. There is then one mass set for distance (Fig. 1) and one for angle for each sensor. There will be another set, based on speed, with the Doppler radar.

The next step consists in combining the distance, angle and speed mass sets for each sensor, and then combining the various sensors. For data fusion, the evidence theory is used with Dempster's conjunctive operator and normalisation.

At the end of those two fusion steps, the mass sets obtained are the number of possible relations between objects. It is now necessary to decide which are the recognized objects, those that appear and those that disappear. This stage is described in the next section.

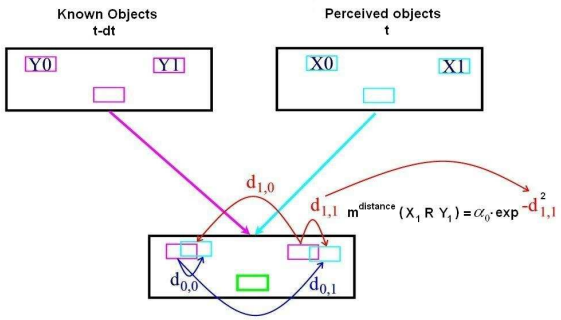

Fig. 1. Association between known and perceived objects using distance information.

4 Object association

When associating objects the decision is taken by means of a fusion algorithm developed by M. Rombaut [24]. This algorithm was improved by D. Gruyer [25].

4.1 Mathematical formulation

The algorithm is based on the calculation of certain masses. The relation mass for a given object i to all the objects j is computed. These masses are noted $m_{i,.}$. The next operation consists in computing the relation masses for each object j to all other i. These masses are noted $m_{.,j}$. The mathematical formulation adopted for $m_{i,.}$ is:

$$\begin{aligned}
m_{i,.}(X_i R Y_j) &= K_{i,.} \cdot m_{i,j}(X_i R Y_j) \cdot \prod_{\substack{k=1 \\ k \neq j}}^{NbK} (1 - m_{i,k}(X_i R Y_k)) \\
m_{i,.}(X_i R *) &= K_{i,.} \cdot \prod_{j=1}^{NbK} m_{i,j}(X_i \overline{R} Y_j) \\
m_{i,.}(\Omega_{i,.}) &= K_{i,.} \cdot [\prod_{j=1}^{NbK} (m_{i,j}(\Omega_{i,j}) + m_{i,j}(X_i \overline{R} Y_j)) - \prod_{j=1}^{NbK} m_{i,j}(X_i \overline{R} Y_j)] \\
K_{i,.} &= \frac{1}{(\prod_{j=1}^{NbK} (1 - m_{i,j}(X_i R Y_j))) \cdot (1 + \sum_{j=1}^{NbK} (\frac{m_{i,j}(X_i R Y_j)}{1 - m_{i,j}(X_i R Y_j)}))}
\end{aligned} \tag{14}$$

Then, $m_{.,j}$ can be deduced:

$$\begin{aligned}
m_{.,j}(Y_j R X_i) &= K_{.,j} \cdot m_{i,j}(X_i R Y_j) \cdot \prod_{\substack{k=1 \\ k \neq i}}^{NbP} (1 - m_{k,j}(X_k R Y_j)) \\
m_{.,j}(Y_j R *) &= K_{.,j} \cdot \prod_{i=1}^{NbP} m_{i,j}(X_i \overline{R} Y_j) \\
m_{.,j}(\Omega_{.,j}) &= K_{.,j} \cdot [\prod_{i=1}^{NbP} (m_{i,j}(\Omega_{i,j}) + m_{i,j}(X_i \overline{R} Y_j)) - \prod_{i=1}^{NbP} m_{i,j}(X_i \overline{R} Y_j)] \\
K_{.,j} &= \frac{1}{(\prod_{i=1}^{NbP} (1 - m_{i,j}(X_i R Y_j))) \cdot (1 + \sum_{i=1}^{NbP} (\frac{m_{i,j}(X_i R Y_j)}{1 - m_{i,j}(X_i R Y_j)}))}
\end{aligned} \tag{15}$$

Note that the non relation masses are not computed. However, this information is not necessary in order to make the decision: deciding that X_i is not in relation with Y_j does not give any information about the other associations.

Two new hypotheses $m_{i,.}(X_i R *)$ and $m_{.,j}(Y_j R *)$ are introduced. In these hy-

potheses, $*$ represents the fact that one object is in relation with none of the others. Thus, if a perceived object X_i is not associated, it is a new object and if a known object is not associated, it has disappeared (masked by another object, out of range, ...). The decision is taken according to the two sets of masses $m_{i,.}$ and $m_{.,j}$. The couples that have the maximum credibility in the two mass set are chosen.

4.2 New formulation

The first remark that can be made about these formulae concerns the framework. At the beginning, when the masses are built, $\Omega_{i,j} = \{(X_i R Y_j); (X_i \overline{R} Y_j)\}$. With the association formulae, it can be seen that Ω changes from a closed world to an extended open world but also that the hypotheses are not the same too: $\Omega_{i,.} = \{(X_i R Y_j); (X_i R *)\}$.

Then, it has been found that in some situations, they did not work well. Indeed, the masses $m_{i,j}(X_i \overline{R} Y_j)$, are added on $m_{i,.}(\Omega_{i,.})$ and $m_{.,j}(\Omega_{.,j})$. While this is not important for the decision because deciding that X_i is not in relation with Y_j does not give any decision, the manner in which the formulae are established adds these masses to Ω and can lead to the choice of a bad decision. For example with one perceived and two known objects the following mass sets are obtained:

$$\begin{array}{ll} m_{1,1}(X_1 R Y_1) = 0.2 & m_{1,2}(X_1 R Y_2) = 0.45 \\ m_{1,1}(X_1 \overline{R} Y_1) = 0.45 & m_{1,2}(X_1 \overline{R} Y_2) = 0.15 \\ m_{1,1}(\Omega_{1,1}) = 0.35 & m_{1,2}(\Omega_{1,2}) = 0.4 \end{array}$$

Therefore:

$M_{cr}^{i,.} =$

	X_1
Y_1	0.121
Y_2	0.396
$*$	0.073
$\Omega_{1,.}$	0.41

$M_{cr}^{.,j} =$

	X_1	$*$	$\Omega_{.,j}$
Y_1	0.2	0.45	0.35
Y_2	0.45	0.15	0.4

From the first matrix ($m_{i,.}$), it can be deduced that the relation on X_1 is unknown: $m_{1,.}(\Omega_{1,.}) = 0.41$ while seeing that $m_{1,.}(X_1 R Y_2) = 0.396$. From the second matrix, it can be decided that Y_1 disappears and that X_1 is in relation with Y_2. So there is a problem with deciding on the couples. To solve

this problem, it was decided to modify the equations for computing the masses $m_{i,.}$ and $m_{.,j}$. This modification consists in defining a unique framework: $\Omega_{i,.} = \{(X_iRY_0); \ldots; (X_iRY_{NbK}); (X_iR*)\}$ and noting $(\overline{X_iRY_j}) = ((X_iRY_k)_{k\neq j} \cup \cdots \cup (X_iR*))$. Thus, the masses are created as follows:

$$\begin{aligned} &m_{i,j}(X_iRY_j) = \alpha_0 \cdot exp^{(-e_{i,j}^2)} \\ &m_{i,j}(\overline{X_iRY_j}) = \alpha_0 \cdot (1 - exp^{(-e_{i,j}^2)}) \\ &m_{i,j}(\Omega_{i,.}) = 1 - \alpha_0 \end{aligned} \tag{16}$$

The masses of relation (X_iRY_j) are increased using the mass on star combined with the complementary masses $(\overline{X_iRY_j})$ that do not contradict the relation hypothesis. The new $m_{i,.}$ values are defined thus:

$$\begin{aligned} m_{i,.}(X_iRY_j) \quad &= K_{i,.} \cdot [m_{i,j}(X_iRY_j) \cdot \prod_{\substack{k=1 \\ k\neq j}}^{NbK} (1 - m_{i,k}(X_iRY_k)) + \sum_{\substack{k=1 \\ k\neq j}}^{NbK} \tfrac{1}{NbK} \cdot m_{i,k}(\overline{X_iRY_k}) \cdot \\ &\prod_{\substack{p=1 \\ p\neq k}}^{NbK} m_{i,p}(\Omega_{i,.}) + \sum_{\substack{k=1 \\ k\neq j}}^{NbK-1} \sum_{\substack{l>k \\ l\neq j}}^{NbK} \tfrac{1}{NbK-1} \cdot m_{i,k}(\overline{X_iRY_k}) \cdot m_{i,l}(\overline{X_iRY_l}) \cdot \\ &\prod_{\substack{p=1 \\ p\neq k, p\neq l}}^{NbK} m_{i,p}(\Omega_{i,.}) + \cdots + \tfrac{1}{2} \cdot m_{i,j}(\Omega_{i,.}) \cdot \prod_{\substack{p=1 \\ p\neq j}}^{NbK} m_{i,p}(\overline{X_iRY_p})] \\ m_{i,.}(X_iR*) \quad &= K_{i,.} \cdot [\prod_{j=1}^{NbK} m_{i,j}(\overline{X_iRY_j}) + \sum_{k=1}^{NbK} \tfrac{1}{NbK} \cdot m_{i,k}(\overline{X_iRY_k}) \cdot \\ &\prod_{\substack{p=1 \\ p\neq k}}^{NbK} m_{i,p}(\Omega_{i,.}) + \sum_{k=1}^{NbK-1} \sum_{l>k}^{NbK} \tfrac{1}{NbK-1} \cdot m_{i,k}(\overline{X_iRY_k}) \cdot m_{i,l}(\overline{X_iRY_l}) \cdot \\ &\prod_{\substack{p=1 \\ p\neq k, p\neq l}}^{NbK} m_{i,p}(\Omega_{i,.}) + \cdots + \sum_{j=1}^{NbK} \tfrac{1}{2} \cdot m_{i,j}(\Omega_{i,.}) \cdot \prod_{\substack{p=1 \\ p\neq j}}^{NbK} m_{i,p}(\overline{X_iRY_p})] \\ m_{i,.}(\Omega_{i,.}) \quad &= K_{i,.} \cdot \prod_{j=1}^{NbK} m_{i,j}(\Omega_{i,.}) \\ K_{i,.} \quad &= \frac{1}{(\prod_{j=1}^{NbK} (1 - m_{i,j}(X_iRY_j))) \cdot (1 + \sum_{j=1}^{NbK} (\frac{m_{i,j}(X_iRY_j)}{1 - m_{i,j}(X_iRY_j)}))} \end{aligned} \tag{17}$$

and the $m_{.,j}$ values:

$$
\begin{aligned}
m_{.,j}(Y_jRX_i) &= K_{.,j} \cdot [m_{i,j}(X_iRY_j) \cdot \prod_{\substack{k=1 \\ k\neq i}}^{NbP} (1 - m_{k,j}(X_kRY_j)) + \sum_{\substack{k=1 \\ k\neq i}}^{NbP} \tfrac{1}{NbP} \cdot m_{k,j}(\overline{X_kRY_j}) \cdot \\
&\quad \prod_{\substack{p=1 \\ p\neq k}}^{NbP} m_{p,j}(\Omega_{.,j}) + \sum_{\substack{k=1 \\ k\neq i}}^{NbP-1} \sum_{\substack{l>k \\ l\neq i}}^{NbP} \tfrac{1}{NbP-1} \cdot m_{k,j}(\overline{X_kRY_j}) \cdot m_{l,j}(\overline{X_lRY_j}) \cdot \\
&\quad \prod_{\substack{p=1 \\ p\neq k, p\neq l}}^{NbP} m_{p,j}(\Omega_{.,j}) + \cdots + \tfrac{1}{2} \cdot m_{i,j}(\Omega_{.,j}) \cdot \prod_{\substack{p=1 \\ p\neq i}}^{NbP} m_{p,j}(\overline{X_pRY_j})] \\
m_{.,j}(Y_jR*) &= K_{.,j} \cdot [\prod_{i=1}^{NbP} m_{i,j}(\overline{X_iRY_j}) + \sum_{k=1}^{NbP} \tfrac{1}{NbP} \cdot m_{k,j}(\overline{X_kRY_j}) \cdot \\
&\quad \prod_{\substack{p=1 \\ p\neq k}}^{NbP} m_{p,j}(\Omega_{.,j}) + \sum_{k=1}^{NbP-1} \sum_{l>k}^{NbP} \tfrac{1}{NbP-1} \cdot m_{k,j}(\overline{X_kRY_j}) \cdot m_{l,j}(\overline{X_lRY_j}) \cdot \\
&\quad \prod_{\substack{p=1 \\ p\neq k, p\neq l}}^{NbP} m_{p,j}(\Omega_{.,j}) + \cdots + \sum_{i=1}^{NbP} \tfrac{1}{2} \cdot m_{i,j}(\Omega_{.,j}) \cdot \prod_{\substack{p=1 \\ p\neq i}}^{NbP} m_{p,j}(\overline{X_pRY_j})] \\
m_{.,j}(\Omega_{.,j}) &= K_{.,j} \cdot \prod_{i=1}^{NbP} m_{i,j}(\Omega_{.,j}) \\
K_{.,j} &= \frac{1}{(\prod_{i=1}^{NbP} (1 - m_{i,j}(X_iRY_j))) \cdot (1 + \sum_{i=1}^{NbP} (\frac{m_{i,j}(X_iRY_j)}{1 - m_{i,j}(X_iRY_j)}))}
\end{aligned}
\tag{18}
$$

In the terms of relation, coefficients appear: $(\frac{1}{NbK}, \ldots, \frac{1}{2})$ for $m_{i,.}$ and $(\frac{1}{NbP}, \ldots, \frac{1}{2})$ for $m_{.,j}$. These correspond to an equal distribution of the mass when there are one or more masses on Ω multiplied with the non relation masses. Indeed, with one perceived and two known objects, if $m_{1,2}(\overline{X_1RY_2}) = (m_{1,1}(X_1RY_1) \cup m_1(X_1R*))$ is multiplied by $m_{1,1}(\Omega_{1,.})$, this means that it is certain that X_1 is not in relation with Y_2. So as the framework is exhaustive and closed, the result goes on $m_{1,.}(X_1RY_1)$ and $m_{1,.}(X_1R*)$ (multiplied by $\frac{1}{2}$). In the case of three known objects, if there are two masses on Ω in the product $(m_{1,1}(\overline{X_1RY_1}) \cdot m_{1,2}(\Omega_{1,.}) \cdot m_{1,3}(\Omega_{1,.}))$, it is not possible to decide where the mass should go, so $\frac{1}{3}$ goes to the first relation $(m_{1,.}(X_1RY_2))$, $\frac{1}{3}$ to the second $(m_{1,.}(X_1RY_3))$ and $\frac{1}{3}$ to the mass on star $(m_{1,.}(X_1R*))$, and so on until divided by NbK (or NbP). Considering the example again, this gives:

$M_{i,.} =$

	X_1
Y_1	0.15
Y_2	0.495
$*$	0.201
$\Omega_{1,.}$	0.154

$M_{.,j} =$

	X_1	$*$	$\Omega_{.,j}$
Y_1	0.2	0.45	0.35
Y_2	0.45	0.15	0.4

This time, there is no ambiguity about the best decision which is: $(X_1 R Y_2)$ and Y_1 disappears. The next section compares the two formulae using synthetic and real data.

5 Experimental results

The aim of this section is to validate the association formulae made using results obtained from simulated or real data. The first part illustrates the use of the formulae[2] with synthetic data and a limited uncertainty, and then with a strong uncertainty. The second part shows the results obtained with real data.

5.1 Synthetic data

5.1.1 With limited uncertainty

In this section, the data were artificially created and the association matrices are not shown. The relevant masses are displayed in order to be able to decide the association as the results are known in advance. The first step was to define a trajectory for the objects (Fig. 2). The objects move for $10s$, with a sample time of $0.1s$, according to the following equations (which introduce strong constraints while remaining realistic):

$$\begin{aligned} &\text{Object } 0 \rightarrow \quad d = \tfrac{1}{2} \cdot 0.1 \cdot t^2 + 5 \cdot t + 19.3 \\ &\text{Object } 1 \rightarrow \quad d = \tfrac{45}{1+exp^{(-2 \cdot t+10)}} + 10 \end{aligned} \tag{19}$$

From these data, the distances between perceived and known objects (Section 3) are computed at each sample time, so as to plot the variation of the

[2] In order to make the computational stage easier, in this part, i ranges from 0 to $NbP - 1$, and j from 0 to $NbK - 1$

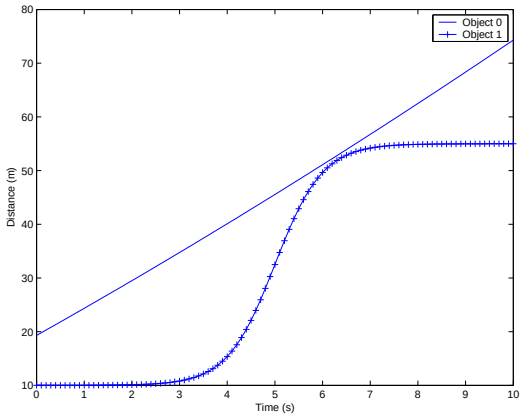

Fig. 2. Variation in object distance from the sensor, for $10s$.

relation masses between those objects (Fig. 3). As the relative distances are not very high, a reliability $\alpha_0 = 0.8$ was chosen for the sensor 0 and $\alpha_1 = 0.8$ for sensor 1. As shown in this figure, the objects are well separated until the moment object 1 approaches object 0 ($5.8s < t < 6.8s$). During this time, $m_{0,1}(\overline{X_0 R Y_1})$ falls whereas $m_{0,1}(X_0 R Y_1)$ increases. However, $m_{0,1}(\overline{X_0 R Y_1})$ is still higher than $m_{0,1}(X_0 R Y_1)$.

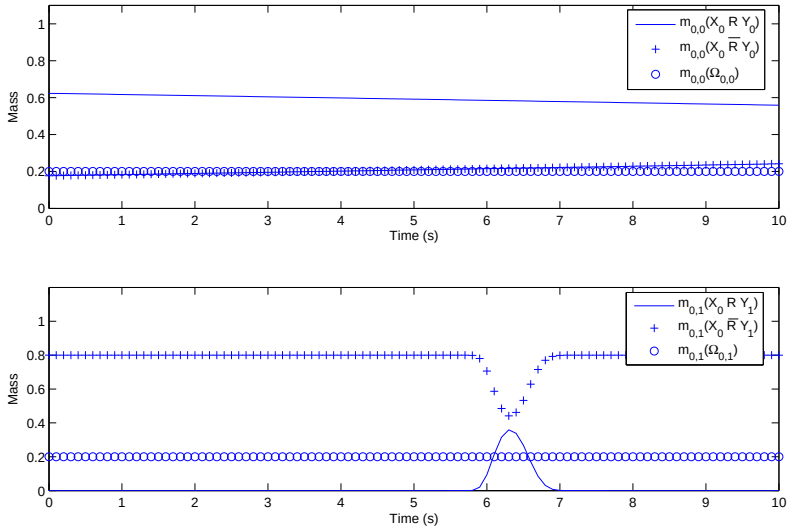

Fig. 3. Variation in relation masses between X_0 and Y_0, X_0 and Y_1.

Figure 4 shows the variation of the association masses using M. Rombaut's formulae. These formulae give good results in this case. In fact, they work well in most cases.

Note that on figure 5 the changes have made to these formulae also give good results. A peak can be seen on $m_{0,.}(\Omega_{0,.})$ (Fig. 5). This variation of mass does not come from the $m_{i,j}(\Omega_{i,j})$ (because these masses are constant with time (Fig. 3)) but from the variation of the conflict coefficient.

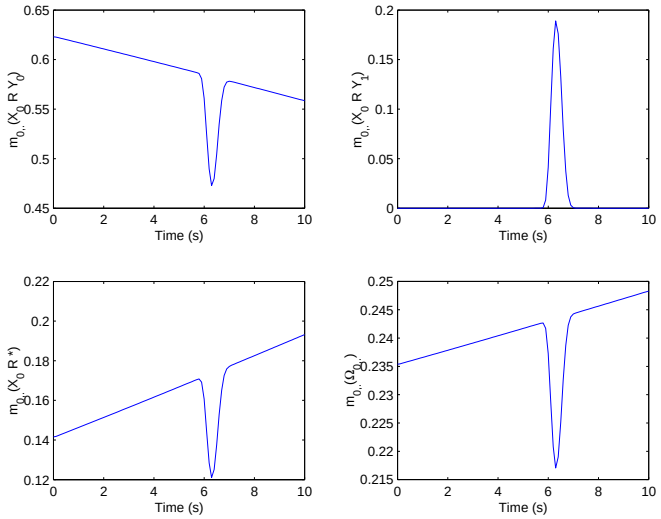

Fig. 4. Variation in $m_{0,.}$ using Rombaut's formulae.

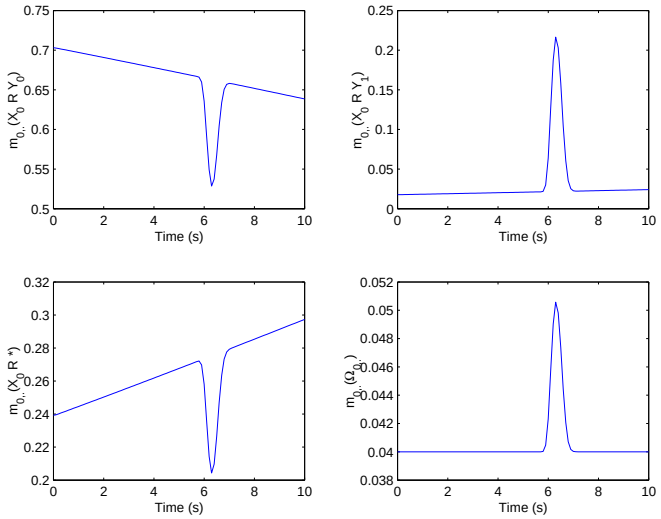

Fig. 5. Variation in $m_{0,.}$ using the modified formulae.

The next part shows the advantage of the modified formulae in the case of low reliability.

5.1.2 With high uncertainty

This is a particular case (Fig. 6) where the temporal equations are:

$$\begin{aligned} \text{Object } 0 \rightarrow \quad & d = \tfrac{1}{2} \cdot 0.1 \cdot t^2 + 5 \cdot t + 59.3 \\ \text{Object } 1 \rightarrow \quad & d = \tfrac{45}{1+exp^{(-2 \cdot t+10)}} + 50 \end{aligned} \tag{20}$$

For this simulation, distances were greater than $50m$, $\alpha_0 = 0.6$ and $\alpha_1 = 0.7$

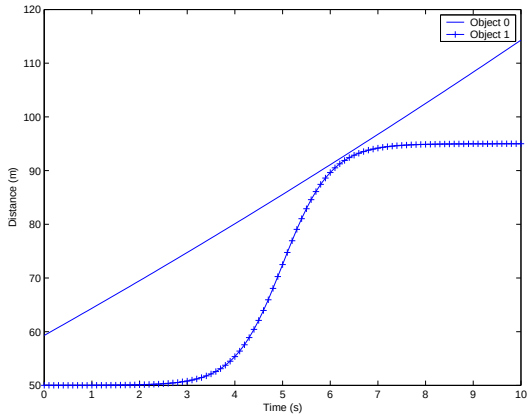

Fig. 6. Variation in object distance, from the sensor, for $10s$.

were fixed. The variation of relation masses is represented on figure 7.

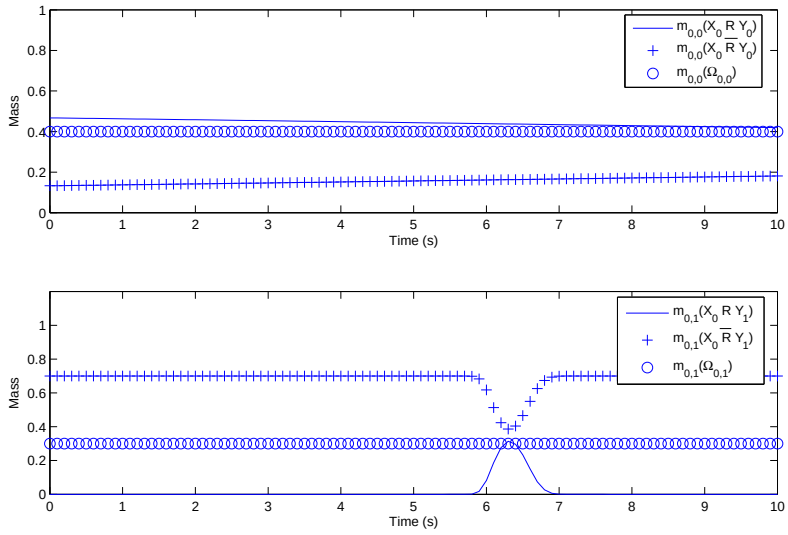

Fig. 7. Variation in relation masses between X_0 and Y_0, X_0 and Y_1.

Figure 8 shows the evolution of association masses using M. Rombaut's formulae. Normally, it should be decided that X_0 is in relation with Y_0. But in this case, it can be seen on the curves that till the beginning the decision of association is debatable. Indeed, the relation mass $m_{0,.}(X_0RY_0)$ is only slightly higher than $m_{0,.}(\Omega_{0,.})$ for $t < 5.8s$ and becomes slightly lower when $t > 5.8s$.

Now, looking at the variation in masses obtained with the modified formulae (Fig. 9), it can be seen that the decision is not ambiguous: X_0 is in relation with Y_0, and this decision is not debatable at any time even when the two objects are very close.

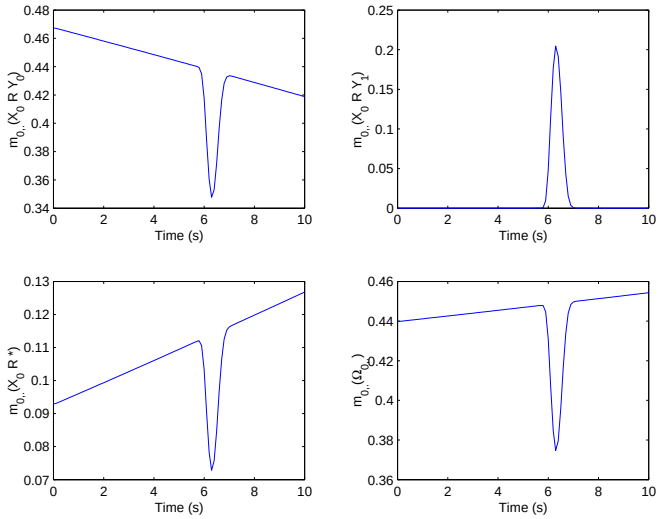

Fig. 8. Variation in $m_{0,.}$ using Rombaut's formulae.

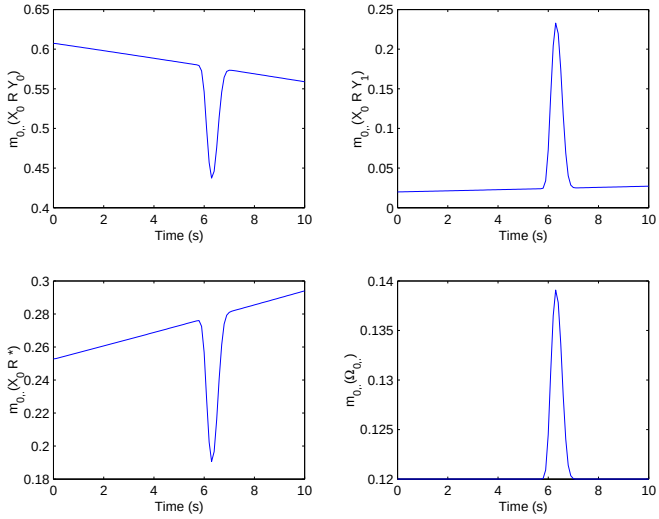

Fig. 9. Variation in $m_{0,.}$ using the modified formulae.

5.1.3 Variation in relation masses according to reliability

For this test, two objects are considered side by side with the same speed and $1m$ apart. Those two vehicles move away progressively from the sensor (from 20 to $100m$ with a constant speed of $5m.s^{-1}$) which leads to a reduction in the reliability coefficient (from 0.9 at $20m$ to 0.3 at $100m$). Figure 10 represents the evolution of the decision reliability according to the sensor reliability for M. Rombaut's algorithm and for the modified one. The decision is not considered to be completely reliable when the variation between the mass of a good decision and another one is lower than a threshold which have been set to 0.1 in this case.

When the reliability is greater than 0.69, the two algorithms give the same

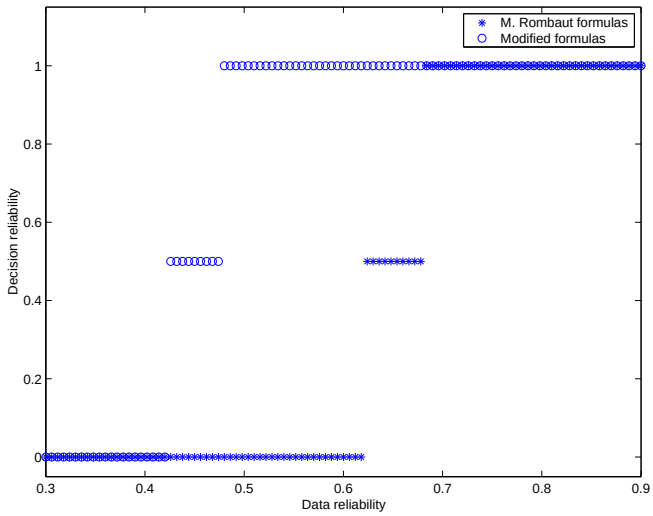

Fig. 10. Variation in the decision reliability according to data reliability.

results. However, the modified algorithm is able to give a reliable decision down to a data reliability value of 0.49. For Rombaut's algorithm, the decision is not reliable below 0.69 and is false if the data reliability value falls below 0.62.

Tests were conducted with a large number of threshold values, always resulting in the same conclusion: the modified algorithm is better when the reliability decreases.

When real tests could be made, it would be interesting to plot the percentage of good decisions of the two algorithms with various data reliability values from several scenarios.

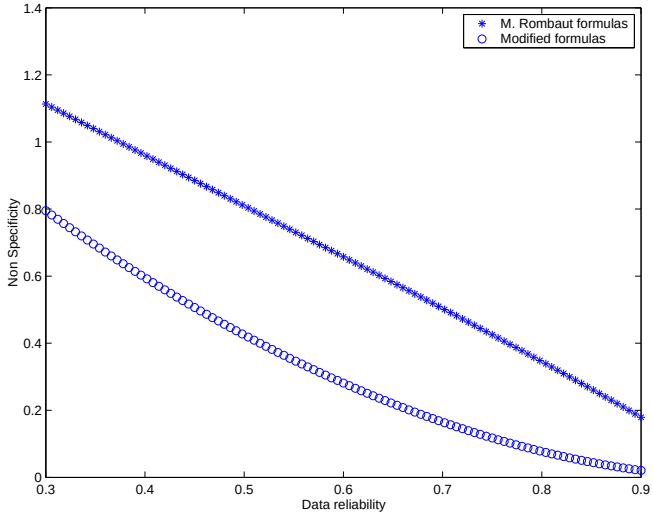

Fig. 11. Variation in the non specificity according to reliability.

Figure 11 shows the variation in non specificity according to data reliability. This figure shows that the modified formulae give more specific mass sets, so

there is less uncertainty on the best decision. These results prove that the modified formulae presented lead to a better decision.

5.2 Real data

The association algorithm was initially tested by using a simulator developed by the authors [26]. This simulator provided the only data that could be used. It was able to create various scenarios thanks to adjustable parameters such as: number and speed of vehicles, number of sensors, sweeping time, angle, range, etc. The driver's behaviour was governed by the driving law. The problem with this simulator was that data were synthetic, so not representative of the driver's behaviour and not noisy. In order to improve the association algorithm and to test its robustness, it was decided to use real data. These data were supplied by a simple DV camera placed behind the windshield of a car. This DV camera has a CCD sensor. The resolution is 720x576 pixels, the angle ranges from -0.5 to $+0.5$ radians (almost $\pm 30°$) and works at 25 images per second ($\Delta_t = 0.04s$). For calibration purposes, a sequence was film in a car park where a reference car was parked. A pocket laser telemeter was used to measure the distance between the camera and the car. The measurements were taken from 0 to $60m$, because for greater distances, it was difficult to point the laser on the car. From the calibration sequence, while assuming that detected objects are cars, two equations were computed by two different interpolation methods (Fig. 12) giving the distance according to object height and width in the image. The angle is extracted from the centre of gravity position in the image. In this way, information (ρ, Θ), for two different sensors is obtained[3].

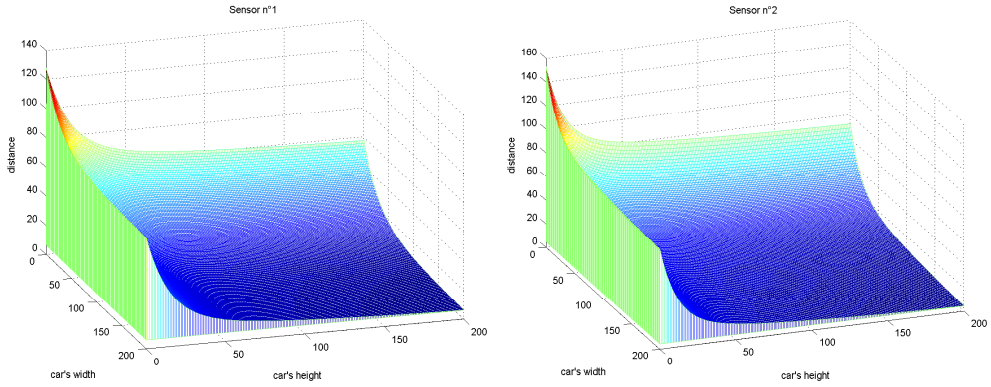

Fig. 12. Characterization function of the two cameras. The distance in meter is obtained from the height and the width in pixels of the object.

[3] The fact of using two different interpolation methods leads to two sources of information. So it can be said that there are two sensors.

Without being specialists in image processing, the measurements extracted were very noisy. Indeed, at $70m$, a variation of $20m$ was possible for the same object from an image to the next. In terms of angle, the variation could be as high as $0.02rd$ for a measurement of $0.01rd$.

5.2.1 Object association

Figure 13 shows the variation in the relation mass for one perceived object. This object is followed for 300 images ($12s$) and is located almost $20m$ from the sensor. The mass of relation varies between 0.57 and 1, but is close to 1 most of the time. A value of 0.57 was obtained because, at this time, there is a measurement error of 14.6% on the distance and a simultaneous 8.2% error on the angle.

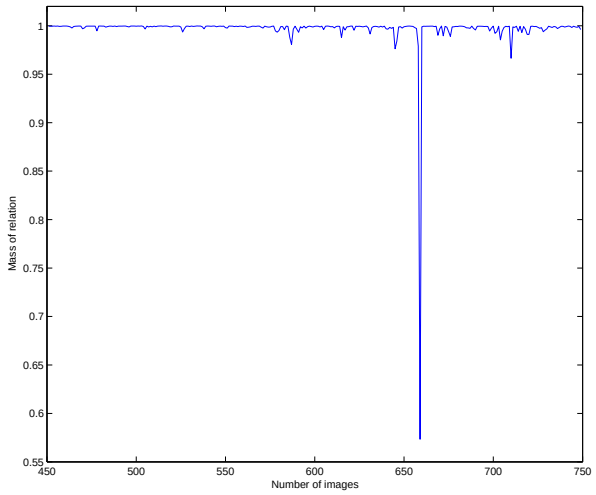

Fig. 13. Variation in the mass of detection for one perceived object.

The entire sequence consists of 3230 images (almost 2min10s) and, during this time, 7063 vehicles were perceived (between 0 and 6 per image). Figure 14 shows the variation in mass on * for the entire simulation using both formulae.

In the scenario presented (Fig. 14) it can be seen that there is many appearance and disappearance of objects (763 during the 3230 images). Note that the masses on star with the new formulae are equal to or higher than the one with Rombaut's formulae. The mass of relation (Fig. 13) is plotted between images 450 and 750. Figure 14 shows that during this time there was just one object and it is always tracked (no appearance or disappearance).

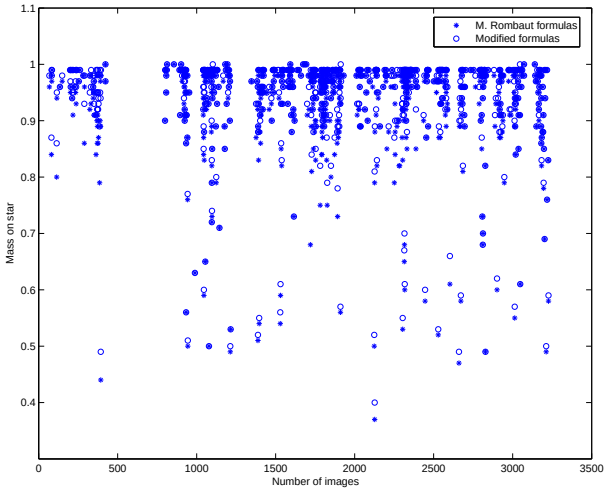

Fig. 14. Variation in mass on * during the entire sequence.

6 Conclusion and future work

This article has presented an improvement to an association algorithm. This algorithm is used to track moving vehicles. Hypotheses to be computed in the association stage have been added in order to reduce the number of ambiguous decisions. This algorithm was tested on synthetic and real noisy data, the maximum variation in distance was about 25% and 200% for the angle from one image to the next. Better results are obtained with the modified formulae especially when the reliability is poor. The number of non-decisions is reduced and the choice of right decision is made easier while increasing the difference between the mass for the best hypothesis and the others.

Improvements could still be made to the detection and tracking of objects by adding a prediction filter to this algorithm. It will thus be possible to predict future associations. This information could then be used to confirm the associations made or reduce the ambiguous decisions on some associations.

References

[1] D. Gruyer, C. Royère, R. Labayrade, and D. Aubert. Credibilistic multi sensor fusion for real time application. application to obstacle detection and tracking. *IEEE International Conference on Advanced Robotics, ICAR'2003, University of Coimbra, Portugal*, June 2003.

[2] A. Broggi, M. Bertozzi, A. Fascioli, C.G.L. Bianco, and A. Piazzi. Visual perception of obstacles and vehicles for platooning. *IEEE Transactions on Intelligent Transportation Systems*, 1(3):164–176, September 2000.

[3] A. Bensrhair, M. Bertozzi, A. Broggi, P. Miché, S. Mousset, and G. Toulminet. A cooperative approach to vision based vehicle detection. In *IEEE International Conference on Intelligent Transportation Systems, ITSC'01*, pages 209–214, August 2001.

[4] C. Stiller, J. Hipp, C. Rössig, and A. Ewald. Multi-sensor obstacle detection and tracking. *Image and Vision Computing*, 18:389–396, 1999.

[5] T. Kato, Y. Ninomiya, and I. Masaki. An obstacle detection method by fusion of radar and motion stereo. *IEEE Transactions on Intelligent Transportation Systems*, 3(3):182–188, September 2002.

[6] M. Bertozzi, A. Broggi, and A. Fascioli. Vision-based intelligent vehicles : state of the art and perspectives. *Elsevier Robotics and Autonomus Systems*, 32(1):1–16, June 2000.

[7] A. Dempster. Upper and lower probabilities induced by multivalued mapping. *Annals of Mathematical Statistics*, AMS-38:325–339, 1967.

[8] G. Shafer. *A Mathematical Theory of Evidence*. Princeton University Press, Princeton, New Jersey, 1976.

[9] P. Smets. What is dempster-shafer's model ? In R.R. Yager, M. Fedrizzi, and J. Kacprzyk, editors, *Advances in the Dempster-Shafer Theory of Evidence*, pages 5–34. Wiley, 1994.

[10] P. Smets and R. Kennes. The transferable belief model. *Artificial Intelligence*, 66(2):191–234, 1994.

[11] R. Kennes and P. Smets. *Uncertainty in Artificial Intelligence*, chapter Computational aspect of the Möbius transformation, pages 401–416. Elsevier Science Publishers, 1991.

[12] R. Kennes. Computational aspects of the möbius transformation of graphs. *IEEE Transactions on Systems, Man and Cybernetics*, 22:201–223, 1992.

[13] P. Smets. The combination of evidence in the transferable belief model. *IEEE Transactions on Pattern Analysis and Machine Intelligence*, 12(5):447–458, 1990.

[14] L. Zadeh. Fuzzy sets and information granularity. In R.K. Ragade, M.M. Gupta, and R.R. Yager, editors, *Advances in Fuzzy Sets Theory and Applications*, pages 3–18. North-Holland Publishing Co., 1979.

[15] R.R. Yager. On the dempster-shafer framework and new combination rules. *Information Sciences*, 41:93–138, 1987.

[16] D. Dubois and H. Prade. A set-theoric view of belief functions: Logical operations and approximations by fuzzy sets. *International Journal of General Systems*, 12:193–226, 1986.

[17] E. Lefevre, O. Colot, P. Vannoorenberghe, and D. de Brucq. Informations et combinaison : les liaisons conflictuelles. *Revue Traitement du Signal*, 18(3):161–177, 2001.

[18] E. Lefevre, O. Colot, and P. Vannoorenberghe. Belief function combination and conflict management. *Information Fusion*, 3(2):149–162, 2002.

[19] G.J. Klir. *Measures of Uncertainty in the Dempster-Shafer Theory of Evidence*, pages 35–49. Advances in the Dempster-Shafer Theory of Evidence. John Wiley and Sons, New York, r.r. yager and m. fedrizzi and j. kacprzyk edition, 1994.

[20] A. Ramer. Uniqueness of information measure in the theory of evidence. *Fuzzy Sets and Systems*, 24(2):183–196, 1987.

[21] G. Klir and A. Ramer. Uncertainty in the dempster-shafer theory : a critical re-examination. *International Journal of General Systems*, 18(2):155–166, 1990.

[22] M. Rombaut and V. Cherfaoui. Decision making in data fusion using dempster-shafer's theory. In *3th IFAC Symposium on Intelligent Components and Instrumentation for Control Applications*, Annecy, France, 9-11 June 1997.

[23] T. Denoeux. A k-nearest neighbour classification rule based on dempster-shafer theory. *IEEE Transactions on Systems, Man and Cybernetics*, 25(5):804–813, 1995.

[24] M. Rombaut. Decision in multi-obstacle matching process using the theory of belief. In *AVCS'98*, pages 63–68, 1998.

[25] D.Gruyer, C.Royère, and V. Cherfaoui. Credibilist multi-sensors fusion for the mapping of dynamic environnement. In *Thrid International Conference on Information Fusion (FUSION'2000)*, page TuC2, 2000.

[26] Y. Lemeret, E. Lefevre, and D. Jolly. Simulator of obstacle detection and tracking. In G. Attiya and Y. Hamam, editors, *5th EUROSIM Congress on Modelling and Simulation*, September 2004.